

Recombinant Oncolytic Vaccinia Viruses Expressing Human β -Defensin 2 Enhance Anti-tumor Immunity

Ting Sun,^{1,5} Yanxi Luo,^{1,5} Minglong Wang,^{2,3} Tian Xie,⁴ and Hui Yan¹

¹Institute of Materia Medica, Zhejiang Academy of Medical Sciences, Hangzhou 310013, China; ²Department of Surgical Oncology, The First Affiliated Hospital, School of Medicine, Zhejiang University, Hangzhou 310003, China; ³Key Laboratory of Precision Diagnosis and Treatment for Hepatobiliary and Pancreatic Tumor of Zhejiang Province, First Affiliated Hospital, Zhejiang University School of Medicine, Hangzhou 310003, China; ⁴Holistic Integrative Pharmacy Institutes, Hangzhou Normal University, Hangzhou 311121, China

Cancer is still a leading of cause of death worldwide. Among the bio-therapy strategies for cancer, vaccinia virus (VV) has been widely used as an expression vector because of its potent oncolytic activities in addition to its large capacity for insertion of foreign genes and excellent safety records. In the present study, a novel recombinant VV, VV-HBD2-lacZ, expressing human β -defensin 2 (HBD2), an anti-microbial peptide of the innate immune system, was constructed. First, the chemotaxis characteristics of HBD2 expressed on VV-HBD2-lacZ-infected cells toward dendritic cells (DCs) *in vitro* and *in vivo* were demonstrated. The anti-tumor effects of VV-HBD2-lacZ *in vitro* and *in vivo* in a mouse melanoma cancer model were then investigated. It was found that VV-HBD2-lacZ was able to inhibit tumor growth and metastasis significantly. It was further demonstrated that VV-HBD2-lacZ induced potent cytotoxic activity by increasing the tumor-infiltrating CD4⁺ and CD8⁺ T cells. These results indicate that HBD2-expressing VV recruited plasmacytoid DCs (pDCs) to the tumor location, leading to cytotoxic T cell response against the tumor, and thus inhibited tumor growth *in vitro* and *in vivo*. In conclusion, oncolytic HBD2-expressing VV provides an effective treatment for tumors by triggering innate and adaptive immunity.

INTRODUCTION

Today, cancer is still a threat to human health, accounting for 8.8 million deaths in 2015.^{1,2} However, traditional cancer therapies have limitations, such as resistance to chemotherapy and radiotherapy as well as poor tumor targeting. On the other hand, post-operative recurrence in some cancers is still a challenging issue that needs to be addressed. With the continuous progress in medical immunology, genetic engineering, and cell and molecular biology, oncolytic virotherapy is a novel therapy strategy for cancer that has attracted increased interest in both research and clinical settings.^{3,4}

Oncolytic virotherapy offers a novel weapon for fighting cancers.^{5,6} Among the oncolytic virotherapy, vaccinia viruses (VVs) have been widely used to prepare cancer vaccines and cancer gene therapy⁷⁻⁹ because of their unique features.^{10,11} Compared with other virus vec-

tors, VVs are potent oncolytic agents that can be administered systematically and spread between tumors within a host.¹² Western Reserve (WR) strain is a replication-competent VV strain that highly selectively infects and lyses tumor cells.¹³ Thorne et al.¹³ compared 10 strains of VV and found that the WR strain displayed greater inherent tumor selectivity *in vitro* than all other strains, primarily due to its enhanced replication in the tumor cell lines. In current clinical trials, VV treatment has shown significant anti-tumor effects. JX-549, a recombinant VV that actively expresses granulocyte-macrophage colony-stimulating factor (GM-CSF), is undergoing phase III clinical trials.^{14,15}

Defensins are a class of small cationic proteins comprising of six to eight conserved cysteine residues. They are, and function as, host defense peptides. Human defensins can be divided into two categories: alpha (α -) and beta (β -)defensins. Human β -defensins (HBDs) are small host defense peptides that play an important role in the defense against various pathogens, and they are considered as a part of the immune system.^{16,17} In addition to their anti-microbial activity, the ability of HBDs to chemoattract and activate immature dendritic cells (DCs) and memory T cells has been reported.^{18,19} Furthermore, the recruitment of DCs also facilitates antigen uptake, processing, and presentation, leading to activation of immune responses. Thus, HBDs play roles in both the innate and antigen-specific immunity of the host.²⁰

In the present study, we constructed a recombinant VV-HBD2-lacZ expressing both HBD2 protein and β -galactosidase (lacZ) as a selective marker to test its anti-tumor effects. The novel recombinant VV exhibited effective therapeutic effects and safe in mouse cancer model. It was further shown that the expression of HBD2 in VV vectors

Received 19 November 2018; accepted 26 March 2019;
<https://doi.org/10.1016/j.omto.2019.03.010>

⁵These authors contributed equally to this work.

Correspondence: Hui Yan, Institute of Materia Medica, Zhejiang Academy of Medical Sciences, Hangzhou 310013, China.

E-mail: yanhui@zjams.com.cn



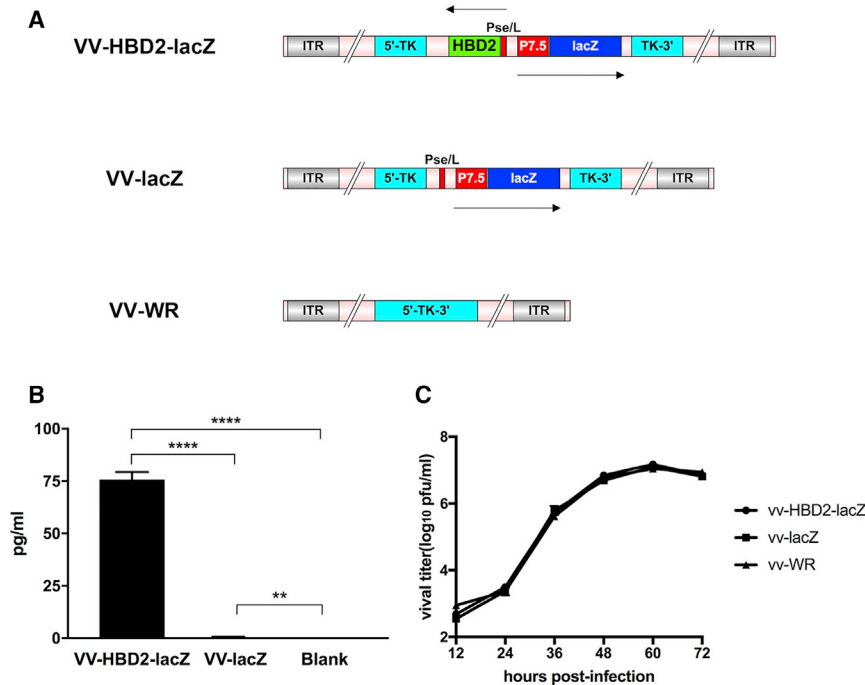


Figure 1. Construction and Characterization of Recombinant VVs

(A) Schematic figure of the genomic structure of recombinant viruses is shown. (B) High expression of HBD2 *in vitro*. A549 cells were infected with VV-HBD2-lacZ or VV-lacZ for 48 h. The HBD2 expression in the supernatants was measured using the human β -defensin 2 ELISA kit (representative of three separate experiments; $n = 5$). (C) Replication rates of VV-HBD2-lacZ, VV-lacZ, and VV-WR on A549 cells. The viral titers in the supernatants obtained at different times were measured by crystal violet plaque assay, and the titer at each time point is presented as mean \pm SD in triplicate. * $p < 0.05$; ** $p < 0.01$; *** $p < 0.001$; **** $p < 0.0001$. P7.5, promoter 7.5; pSE/L, proximal sequence element promoter; HBD2, human β -defensin 2.

enhanced the innate immune activation and inhibited immunosuppression, resulting in potent anti-tumor immunity.

RESULTS

Construction and Characterization of Recombinant Viruses

In this study, two recombinant VV vaccines were constructed: VV-HBD2-lacZ, expressing both HBD2 and β -galactosidase (lacZ), and VV-lacZ, expressing β -galactosidase only. Genomic structures of VV-HBD2-lacZ, VV-lacZ, and VV-WR are presented in Figure 1A.

Integration of both HBD2 and lacZ sequences into the desired site in the thymidine kinase (TK) region of the virus was confirmed by PCR and sequencing of viral DNA (data not shown).

ELISA analysis showed a high level of HBD2 expression in both human and murine tumor cell lines infected with VV-HBD2-lacZ but not VV-lacZ (Figure 1B). The bioactivity of HBD2 protein was also measured, which included its bacteriostatic activity, based on cells infected with VV-HBD2-lacZ or VV-lacZ. Infected cell lysates were collected and filtered through a 70- μ m filter. Bacteriostatic activity of HBD protein was determined by the agar plate diffusion method. As shown in Table 1, the VV-HBD2-lacZ group displayed significantly more potent bacteriostatic activity than the other groups.

To confirm if recombinant viruses VV-HBD2-lacZ and VV-lacZ as well as wild-type of VV (VV-WR) had a similar pattern of proliferation in tumor cell lines. A549 cells were infected at an MOI of 0.1 with VV-HBD2-lacZ, VV-lacZ, or VV-WR. As shown in Figure 1C, it was found

that the two recombinant viruses had a similar replication rate compared with VV-WR strain.

VV-HBD2-lacZ and VV-lacZ Induce Specific Cancer Cell Death via Apoptosis Pathway

To evaluate the tumor-specific cytotoxicity of VV-HBD2-lacZ and VV-lacZ, several human

and mouse tumor cell lines and non-cancerous cell lines were infected with VV-HBD2-lacZ or VV-lacZ for 48 h. VV-WT group was used as a control. Cell viability was measured by cell counting kit-8 (CCK-8) assay. The results (Figure 2A) showed that the growth of tumor cells infected with TK-deleted recombinant VVs (VV-HBD2-lacZ and VV-lacZ) was inhibited in a dose-dependent manner, while the growth of non-cancerous NIH 3T3 cells infected with either VV was apparently not inhibited. The highest cytotoxicity was found in B16F10 cells, where the cell viability decreased to $12.8\% \pm 3.74\%$ at an MOI of 10 after 48 h of infection. On the contrary, the cell viability of NIH 3T3 cells slightly changed ranging between an MOI of 0.1 and 10. These findings suggest that the TK-deleted recombinant viruses have a specific suppressive effect on tumor cell proliferation but not normal cells.

To figure out whether the expression of HBD2 increases tumor cell death by activating the apoptosis or necrosis pathway, A549 cells and B16F10 cells were treated with VVs for 24 h. The percentage of apoptotic cells was then determined by annexin V/PI and flow cytometry assays. The results analyzed by flow cytometry showed that the percentage of cell apoptosis in tumor cells infected by VV-HBD2-lacZ was higher (2-fold) than in the VV-lacZ group (Figure 2B).

VV-HBD2-lacZ Attracts Activated DCs *In Vitro* and *In Vivo*

To determine whether the enhanced anti-tumor effects were related to the chemotactic character of HBD2, a supernatant was collected from VV-HBD2-lacZ- or VV-lacZ-infected cells and DCs were isolated from murine spleen. The chemotactic index of DCs was measured using the coring transwell chamber (5- μ m pore size;

Table 1. Bacteriostatic Activity of HBD2

Groups	Diameter of Inhibition Zone (mm)			
	<i>E. coli</i> DH5 α	<i>E. coli</i> BL21	ZJ111	<i>S. aureus</i>
Amp	24.32 \pm 1.04	24.10 \pm 1.38	26.43 \pm 0.41	29.66 \pm 0.67
VV-HBD2-lacZ (0.2 μ g/mL)	17.11 \pm 0.80	15.24 \pm 0.87	11.06 \pm 0.22	19.26 \pm 0.53
VV-HBD2-lacZ (0.1 μ g/mL)	11.63 \pm 1.31	11.45 \pm 0.54	7.94 \pm 0.11	14.86 \pm 0.43
VV-lacZ	0	0	0	0
PBS	0	0	0	0

Dates are means \pm SD; n = 3 independent experiments. For each experimental repeat, each condition is tested with three plates. Amp, ampicillin.

Costar, London, UK). The results of transwell chemotaxis assay *in vitro* showed that the chemotactic index of the VV-HBD2-lacZ group was nearly 8-fold higher than that of VV-lacZ group (Figure 3A).

To figure out whether VV-HBD2-lacZ attracts DCs into tumors *in vivo*, C57BL/6 mice received intraperitoneal injection of 10^8 plaque-forming units (PFU)/mouse VV-HBD2-lacZ or VV-lacZ, and they were sacrificed after the second dose. The results revealed a higher level of CD11c⁺ CD45RA⁺CD8⁺ plasmacytoid DCs (pDCs) in the tumor of VV-HBD2-lacZ-treated mice (Figure 3B). In summary, VV-HBD2-lacZ have the ability to attract DCs *in vitro* and *in vivo*.

Recombinant VVs Show Potent Tumor Therapeutic Potential in Mouse Melanoma Models

Vector safety is a crucial parameter for the therapeutic use of oncolytic viruses. To determine the safety of recombinant mutant VVs, C57BL/6 mice were injected intraperitoneally with a dose of 10^9 PFU/mouse recombinant VVs, while the control group was injected with 10^6 PFU/mouse of VV-WR. The results showed that 10^6 PFU/mouse VV-WR was lethal to the control mice, whereas mice receiving recombinant VVs showed a slight body weight loss that increased again at day 6 (Figure 4A). In addition, VV-WR-treated mice were all sacrificed at day 10 due to being moribund, while 100% of the mice treated with TK-deleted viruses survived for at least 30 days (Figure 4B).

Biodistribution studies of VV-HBD2-lacZ or VV-lacZ showed that the biodistribution pattern of VV-HBD2-lacZ and VV-lacZ were similar. As demonstrated, there was no significant difference in viral titers among the tissues at day 3 when comparing VV-HBD2-lacZ with VV-lacZ. The viral titer in organs other than the tumor began to decrease sharply at day 6; on the contrary, it was found that almost all recombinant VVs accumulated in the tumor tissue after day 9 in contrast with normal organs, where only few traces were detected (Figure 4C).

A mice model was used to evaluate the anti-tumor effects of VV-HBD2-lacZ and VV-lacZ based on the hypothesis that VV-expressed

HBD2 may attract mouse DCs into the tumor location²¹ *in vivo*. VV-HBD2-lacZ, VV-lacZ (10^9 PFU/mouse), and PBS were then injected, respectively, into tumor *in situ* in B16F10 tumor-bearing mice (Figure 5A). The injections were then repeated at day 12 and day 17. It was found that treatments with VV-HBD2-lacZ and VV-lacZ inhibited the growth of established tumors ($p < 0.0001$; $p < 0.001$) (Figures 5B and 5C) and prolonged the survival period of tumor bearing-mice compared with the PBS-treated group (Figure 5D). All mice inoculated with PBS were sacrificed at day 19 when the tumor volume reached 2000 mm³, while the mice inoculated with VV-HBD2-lacZ and VV-lacZ showed 80% and 100% survival, respectively, at day 25.

To test whether VV-HBD2-lacZ could increase systemic anti-tumor response, the VV-treated mice were re-challenged with another dose of 10^5 B16F10 cells/mouse on the other flank 2 weeks after the first injection. The results suggested that VV-HBD2-lacZ-treated mice had great resistance to B16F10 cell re-challenge compared to VV-lacZ treated mice (Figure 5E).

VV-Expressing HBD2 Enhances Therapeutic Effects *In Vivo* by Inducing Cytotoxicity T Cell Responses

To explore the immune responses induced by HBD2 protein, tumor tissues were collected and stained with anti-mouse CD4 and anti-mouse CD8 and analyzed by fluorescence-activated cell sorting (FACS) assay. As expected, the percentage of CD4⁺CD8⁺ T cells was significantly increased in the tumor of VV-HBD2-lacZ-treated mice (Figure 6B). A significant increase was observed in the number of CD4⁺ (45.8%) and CD8⁺ (30.2%) T cells in the VV-HBD2-lacZ-treated group compared with the VV-lacZ-treated group. Splenocytes were also co-cultured with tumor cells to assess the tumor-specific cytotoxic T lymphocyte (CTL) activity *in vitro*. As shown in Figure 6A, Splenocytes from VV-HBD2-lacZ mice had higher cytotoxicity than VV-lacZ and PBS-vaccinated mice at different effector:target ratios. These findings indicate that VV-HBD2-lacZ can induce and enhance tumor-specific immune responses.

To ascertain that the CTL activity was mediated by CD8⁺ cells, *in vitro* antibody blocking experiments were carried out. Cytotoxic activity of splenocytes targeted to tumor cells was tested after co-culture of splenocytes with monoclonal antibodies against CD8 molecules. The results demonstrated that the CTL activity was most likely primarily mediated by CD8⁺ T cells because the specific lysis was significantly inhibited in CD8-block group and the inhibition of anti-CD8 antibody was more than 90% (Figure 6C).

To determine the type of immune cell required for the therapeutic functions of HBD2 in the melanoma model, antibody depletion experiments were performed *in vivo*. 10^5 B16 melanoma cells were implanted interdermally in C57BL/6 mice. Seven days after tumor implantation, the mice were treated with anti-CD4, anti-CD8, and anti-CD4 + anti-CD8 before intratumoral injection of viruses. This was repeated twice per week until the mice died or up to the 25th day. It was found that depletion of CD4⁺ or CD8⁺ T cells resulted

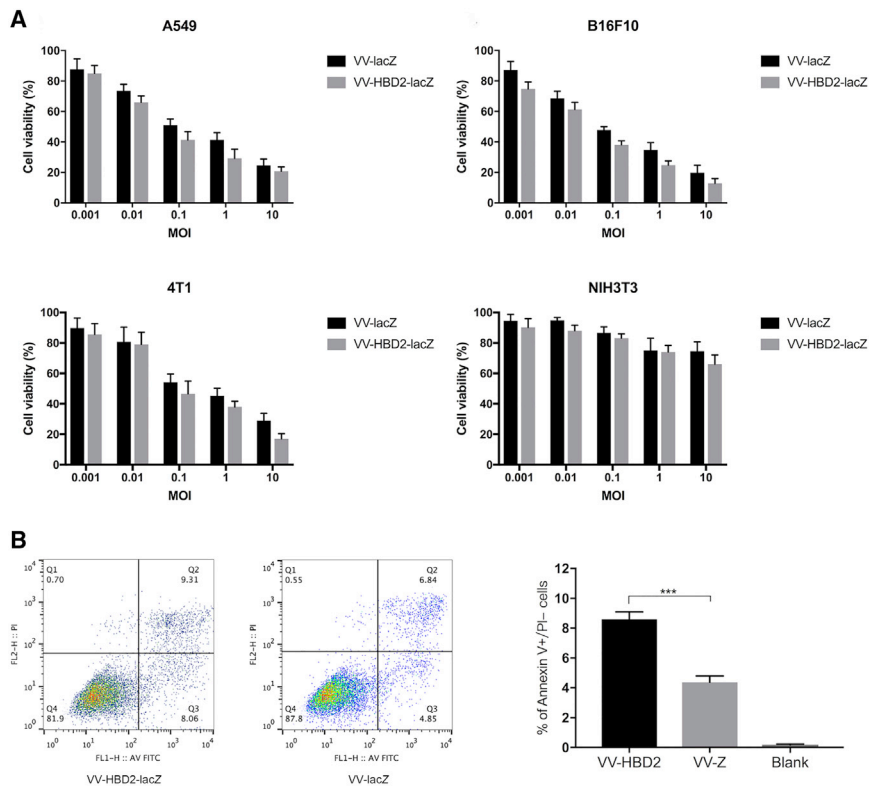


Figure 2. VV-HBD2-lacZ and VV-lacZ Induce Tumor Cell Death Specifically

(A) One human tumor cell, two murine tumor cells, and one murine normal cell were infected with VV-HBD2-lacZ or VV-lacZ for 48 h. Cell viability was measured by cell counting kit-8 (CCK-8) assay. Data is presented as mean \pm SD of three separate experiments. (B) The cell apoptosis induced by recombinant viruses at an MOI of 1 for 24 h was detected by an annexin V/PI-staining kit and flow cytometry.

vation of DCs elicits potent anti-tumor immunity. However, ELISA results showed that adenovirus vector expresses a low level of BD2 proteins.

Inspired by the above studies, a novel TK-deletion recombinant VV was generated in this study by inserting the exogenous gene *HBD2* into the TK region of the VV-WR strain. It was also shown here that recombinant VVs with the deletion of the *TK* gene were preferentially toxic to tumor cell lines and were safe in normal cell lines (Figure 2A), because only cancer cells contain high concentrations of functional nucleotides that enable VVs to replicate after the deletion of viral thymidine kinase.²⁷ Thus, the results in this work support the concepts that TK-deleted VVs preferentially replicate in tumor cells but replicate poorly in normal cells.²⁸ This study further explores the tumor targeting of recombinant VVs by assaying the viral titer in different cell lines (Figure 4A).

In addition, the analysis of ELISA results showed that VVs can highly express HBD2 at the tumor site, which may enhance the immunogenicity of tumor antigens released from VV-infected cells and therefore boost immune responses.

This study provides evidences that HBD2 does attract and activate immune cells (pDCs) *in vivo* and *in vitro*. It was found that the main phenotype of immune-cell-infiltrating tumor is CD11c⁺CD45RA⁺CD8⁺ (pDCs) (Figure 3) after VV-HBD2-lacZ vaccination, whereas the immune cells in the tumor of VV-lacZ-infected mice exhibited CD11c⁺CD45RA⁻CD8⁻ phenotype. pDCs is a type of immune cell that is known to secrete large quantities of type 1 interferon (mainly IFN- α and IFN- β) in response to a viral infection.²⁹ IFN- α and IFN- β , which are two potent anti-tumor cytokines in the immune response, can induce and enhance natural killer cells as well as CTL response.^{30,31} Other than conducting antiviral mechanisms, pDCs are considered to be key in linking the innate and adaptive immune systems because they are capable of activating other immune cells.^{32,33} Maturation of pDCs is initiated when the cell comes into contact with a virus, prompting the upregulation of major histocompatibility complex (MHC) class I and MHC class II. Besides,

in increased tumor growth rate (Figure 6D) and shortened the survival (Figure 6E) compared with the non-depletion group. It was also observed that the CD8⁺ T cells were more potent than CD4⁺ T cells in the suppression of melanoma tumor (Figure 6D).

DISCUSSION

Oncolytic virotherapy is a novel and promising treatment approach that has shown great efficacy in anti-tumor clinical trials.^{7,8,22} Oncolytic virotherapy uses replication-competent oncolytic viruses that selectively target, infect, and lyse tumor cells to treat cancers. Thus, compared with traditional treatments, such as chemotherapy and radiotherapy, oncolytic virotherapy is superior in cancer therapy.

VV is an attractive vector for cancer therapy due to its ability to accept large exogenous genes, high immunogenicity, safety, and tumor targeting.^{23,24} Compared with other oncolytic viruses, it also has a rapid replication cycle and high replication efficiency.²⁵

It is well known that HBD2 protein has the ability to chemoattract and activate immune cells to induce systemic immunity, which then enhance immunogenicity of the tumor antigens.^{19,20} Huang et al.²¹ reported that HBD2 was chemotactic for both murine immune cells and human immune cells and presented antigens into the immune system and activated immune response in mouse model. Lapteva et al.²⁶ constructed a recombinant adenovirus encoding β -defensin 2 (BD2) then assessed the chemotactic properties of BD2 in mouse model. They demonstrated that the attraction and acti-

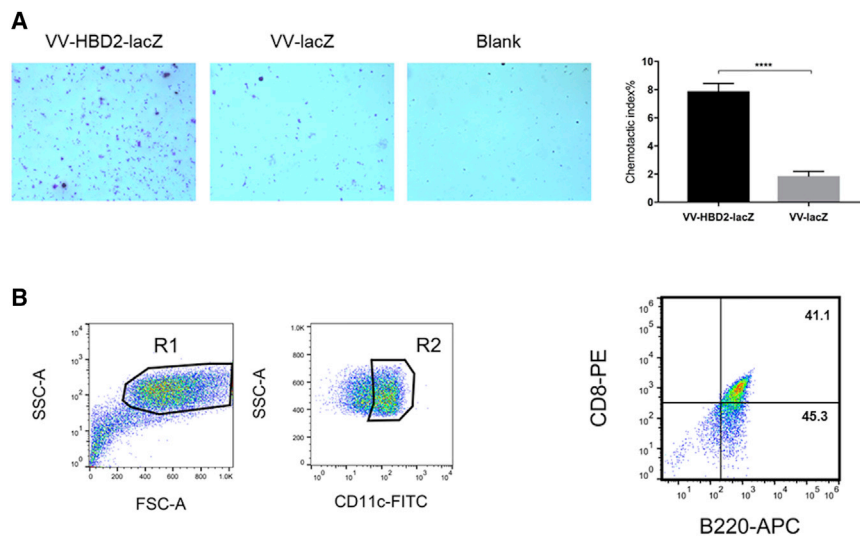


Figure 3. Chemotaxis Characteristics of VV-HBD2-lacZ on DC Cells

(A) *In vitro* chemotaxis activity of VV-HBD2-lacZ or VV-lacZ on activated DCs was detected by transwell assay. The results are presented as mean \pm SD of triplicate samples. The assay was repeated twice. (B) Increased number of pDCs (plasmacytoid dendritic cells) in melanoma tumor of mice vaccinated with VV-HBD2-lacZ. Tumor cells were stained with anti-mouse CD11c, CD45RA, and CD8. Gates were set on CD11⁺ cell population. The percentage of pDCs is presented as mean \pm SD of three separate experiments (n = 3). *p < 0.05; **p < 0.01; ***p < 0.001; ****p < 0.0001. FITC, fluorescein isothiocyanate; APC, allophycocyanin.

MHC class I on pDC surfaces is able to activate CD8⁺ T cells, while MHC class II has been found to activate CD4⁺ T cells.³⁴ In the subsequent study, flow cytometric analysis demonstrated that the percentage of CD4⁺CD8⁺ T cells in tumor cells of VV-HBD2-lacZ-treated mice significantly increases. The results of an *in vitro* cytotoxicity assay demonstrated that the CTL activity was mainly mediated by CD8⁺ T cells. Further support for this hypothesis was seen in CD4⁺ or CD8⁺ antibody-depletion assay *in vitro*. It was found that the CTL activity reduced in CD4⁺ or CD8⁺ block group was reduced. It is therefore clear that the CD4⁺ and CD8⁺ T cells play an important role in tumor suppression.

It was also observed that VV-HBD2-lacZ were more potent in inducing cell apoptosis compared with VV-lacZ. In general, VVs induce cancer cells' programmed necrosis and temporarily inhibit apoptosis for viral replication. However, this work demonstrates that the level of cell apoptosis increased in tumor cells according to flow cytometric analysis. Therefore, it was hypothesized that HBD2 can overbalance necrosis to apoptosis, resulting in achievement of higher tumor specificity and oncolytic activity.

In the B16F10 mouse model, it was observed that VV-HBD2-lacZ and VV-lacZ viruses caused tumor suppression and significantly prolonged survival compared with the control group. VV-HBD2-lacZ caused a more potent and enduring suppression in C57BL/6 mice than VV-lacZ. Thus, it is believed that the VV-HBD2-lacZ is able to attract DC and CTL infiltration into tumors and significantly inhibit tumor growth. In addition, the re-challenging experiments showed that VV-HBD2-lacZ could induce a systemic anti-tumor response to control distant metastatic tumors.

Thus, it was inferred that VV-HBD2-lacZ possibly preferentially infects tumor cells and kills tumor cells by direct oncolysis mechanisms, such as the release of tumor antigens and HBD2 protein, which works as an oncolytic therapy. HBD2 protein then plays a

chemotactic role to attract pDCs, which present tumor antigens to the immune system *in vivo*, thereby inducing the generation of Th1 CD4⁺ helper T cells and CD8⁺ cytotoxic T HBD2 protein, which recruits and activates immune cells into the tumor. This finally triggers immune response and suppresses the growth of tumors.

It is now clear that a recombinant oncolytic virus, VV-HBD2-lacZ, causes tumor suppression by activating the immune system. However, the signaling pathway related to immune responses is still largely unknown. Further studies are needed to demonstrate the mechanisms responsible for these immune responses.

In conclusion, these results suggest that the recombinant oncolytic vaccinia encoding HBD2 protein might be an efficient strategy for boosting immune system and cancer therapy. In addition, further studies needed to be carried out on humanized mouse models using more immunogenic tumors to evaluate the stability of this vaccine.

MATERIALS AND METHODS

Cell Lines and Animals

Murine embryo fibroblast cells (NIH 3T3), HEK293 cells, and African green monkey kidney epithelial cells (Vero) were preserved in our laboratory and cultured in DMEM (Gibco, Thermo Fisher Scientific, Waltham, MA, USA) supplemented with 10% fetal calf serum (FCS). Human alveolar adenocarcinoma cells (A549), murine breast carcinoma cells (4T1) and murine melanoma cells (B16F10) were preserved in our laboratory and cultured in RPMI 1640 (Gibco, Thermo Fisher Scientific, Waltham, MA, USA) supplemented with 10% FCS, penicillin (100 U/mL), streptomycin (100 μ g/mL). All cells were cultured at 37°C at 80% humidity and 5% CO₂.

C57BL/6 male mice (6–8 weeks old) used in this study were purchased from Shanghai SIPPR-BK Lab Animal Co. (Shanghai, China). All animal studies were done under protocols from the Experiment Animal Center, Zhejiang Academy of Medical Sciences, and experiments were approved by the Ethics Committee of Animal Experimentation of Zhejiang Academy of Medical Sciences.

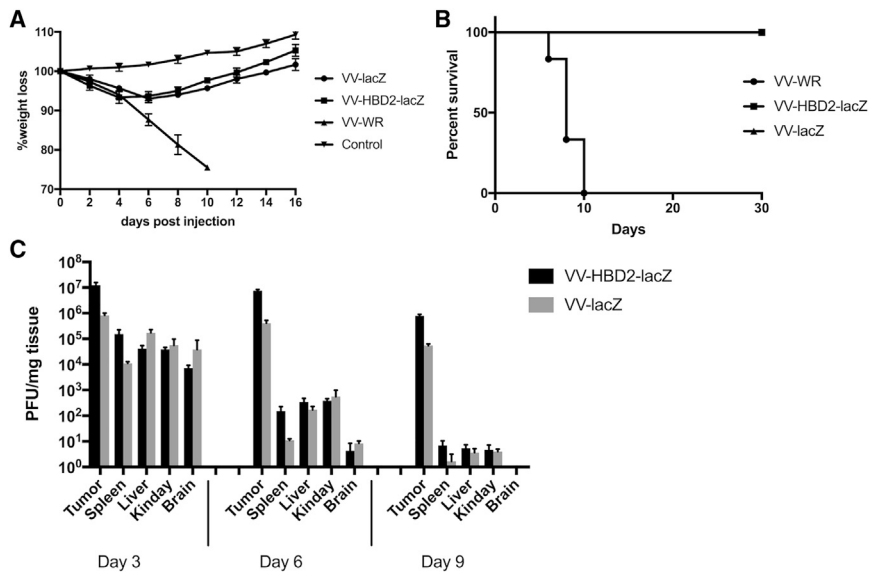


Figure 4. Biodistribution of VV-HBD2-lacZ or VV-lacZ In Vivo

C57BL/6 mice were injected with different virus doses, and body weight loss (A) and survival time (B) were monitored daily. (C) C57BL/6 mice received 5×10^8 PFU/mouse VVs and were sacrificed at day 3, 6, and 9 ($n = 10$). Virus titers in tumor, spleen, liver, lung, and brain were titered by plaque assay. PFU, plaque-forming unit.

sequences were 5'-GACTATGGACGCATGATAAG-3' (Spe I-HBD2) and 5'-CGCGGATCATGAGAGTATTATTTATTATTTTC-3' (HBD2-BmH I) for HBD2. The PCR products were electrophoresed in 1% agarose gel containing ethidium bromide for visualization.

Viral Replication Assay

Cells infected at an MOI of 0.1 were harvested 48 h post-infection (hpi) and subjected to three cycles of freeze-thaw to release the

viruses.¹⁰ The virus was then titered by crystal violet plaque assay in triplicate.

Bacteriostatic Activity

Bacteriostatic activity of HBD protein was determined by the agar disk-diffusion test.³⁵ A549 cells were infected with VV-HBD2-lacZ or VV-lacZ (negative control) for 48 h. Cell lysates were collected after three freeze-thaw cycles and filtered through a 70- μ m filter. *Escherichia coli* (*E. coli*) DH5 α , *E. coli* BL21, ZJ111,³⁶ and *Staphylococcus aureus* (*S. aureus*) were incubated at 37°C to grow to mid-log phase in liquid Luria-Bertani broth (LB) medium and coated on 9 cm² Petri plates. Samples from supernatants of VV-infected cells were loaded into 5-mm wells in the agarose plates and incubated overnight. The inhibition zone around each well was measured to quantify the bacteriostatic activity.

In Vitro Tumor-Cell-Killing Assay

100 μ L cell suspension (5×10^4 cells/well) was seeded in quintuplicate into 96-well plates. After 24 h, 100 μ L recombinant VVs were added to cells and incubated for 48 h at 37°C, 5% CO₂. 100 μ L culture medium was added into five wells of 96-well plates as a blank control. Cell viability was measured using a CCK-8 (Shanghai Sangon Biotech) according to the manufacturer's protocol. The optical density (OD) was measured using a microplate reader (Bio-Tek, Hercules, CA, USA) at 450 nm. Each experiment was repeated at least three times. The percent of cell viability was calculated by (treatment OD – blank control OD)/(negative control OD – blank control OD) \times 100%.

Animal Experiments

For analysis of tumor growth and survival, 1×10^5 B16F10 cells/mouse were subcutaneously injected into the upper right flank of C57BL/6 mice. When the tumor volume increased to 50 mm³, the mice were assigned in a random, blinded manner to divide them

Viruses

The DNA sequences encoding HBD2 (GenBank: AF040153.1) was amplified by PCR using the primer HBD2-Bm (5'-CGC GGA TCC ATG AGA GTA TTA TAT TTA TTA TTT TC-3') and Spe-HBD2 (5'-CGG ACT AGT ATT ATG GTT TTT TAC AAC ATT TAG-3') using a homemade plasmid pUC-HBD2 as template (unpublished data). The PCR products were purified by 1% agarose gel electrophoresis and inserted into pCBlacZ vector. The sequence was confirmed by PCRs and DNA sequencing. The recombinant VVs were generated by homologous recombination of transfer plasmid pCBlacZ or pCB-HBD2-lacZ with VV-WR strains. Plaque purification and Geneticin (G418) were used to select and isolate the TK deletion virus. Recombinant VVs were amplified in A549 cells and purified by sucrose-gradient ultracentrifugation. The purified viruses were titered by crystal violet plaque assay and stored at -80°C .

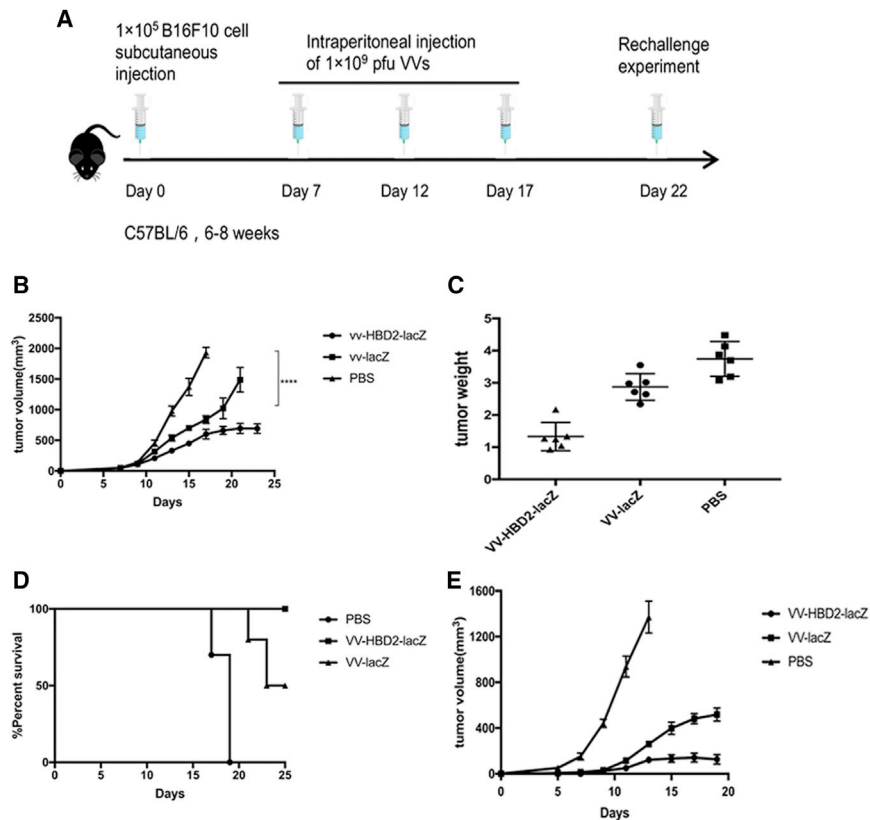
The WR strain wild-type vaccinia was kindly provided by the NIH-AIDS Research & Reference Reagent Program.

ELISA

A549 cells were infected with either VV-HBD2-lacZ or VV-lacZ at an MOI of 0.5 for 48 h. Cell lysates were collected after three freeze-thaw cycles. The expression of HBD2 was measured using the HBD2 enzyme-linked immunosorbent assay kit (Beyotime Biotechnology, Guangzhou, China) according to the manufacturer's instructions. The absorbance was read on an absorption spectrophotometer (Bio-Tek, Hercules, CA, USA) at 450 nm.

PCR

PCR amplification was performed in a volume of 20 μ L containing 1 μ g of cDNA, 1 μ L of each primer, and 10 μ L 2 \times Taq master mix (NEB, USA) under the following reaction conditions: 94°C for 90 s, 30 cycles at 95°C for 30 s, 60°C for 30 s, and 72°C for 35 s. Primer



into three groups and injected intraperitoneally with PBS or 10^9 PFU/mouse VV-HBD2-lacZ or VV-lacZ, respectively. The injections were repeated every 5 days according to the scheme in Figure 5A. The PBS group was used as a control. Tumor volumes ($0.5 \times \text{length} \times [\text{width}]^2$) were monitored every other day, and survival was recorded. Mice were euthanized when the tumor volume reached 2000 mm³.

For the *in vivo* viral bio-distribution experiment, the mice were intraperitoneally injected with 100 μ L 10^8 PFU/mouse VV-HBD2-lacZ or VV-lacZ and sacrificed at 2, 4, 6, 8 or days post-inoculation. Homogenized tissues of VV-treated mice were titered using a crystal violet plaque assay. For re-challenge experiment, C57BL/6 mice received a second 10^5 B16F10 cells/mouse in the left flank 2 weeks after the first inoculation.

Cell Isolation and Generation

Three mice from each group were sacrificed at 5 days after the second injection. Tumors as well as spleens were collected and filtered through a 70- μ m cell strainer (Falcon; Corning). A single-cell suspension was centrifuged at 1,000 rpm for 5 min and lysed using red blood cell lysis buffer.²⁶

Spleen-derived DCs were isolated according to the references described. Cells were cultured in RPMI 1640 with 10% FCS, 20 ng/mL murine GM-CSF (PeproTech, Rocky Hill, NJ, USA), and 10 ng/mL mouse interleukin-4 (mIL-4; PeproTech, Rocky Hill, NJ,

USA) for 6 days. Half of the medium was changed every 2 days, and sufficient amount of GM-CSF and mIL-4 were added. Suspension cells were collected and cultured for 2–3 days in RPMI 1640 medium with 20 ng/mL GM-CSF, 10 ng/mL mIL-4, and 15 ng/mL TNF- α before the assays.

Transwell Chemotaxis Assay

Mature DCs were collected and resuspended in serum-free RPMI 1640 medium.³⁷ Mature DCs or splenocytes were diluted to 2×10^5 cells/well with serum-free medium and seeded into the upper compartment of a microchemotaxis chamber (5 μ m pore size, Costar, London, UK) at 37°C under 5% CO₂. Supernatants collected from infected cells were added to the lower compartment. After 3 h of incubation at 37°C under 5% CO₂, the medium in the upper chamber was removed and washed twice with PBS. The cells were fixed in formaldehyde for 30 min and stained with 0.1% crystal violet and then washed twice with PBS. The cells that had not migrated were scraped off, and the cells that had migrated were counted in five random microscopic fields. Chemotactic index (%) = the number of migrated cells in test group/the number of migrated cells in control group \times 100%.

Flow Cytometry Assay

For detection of apoptosis, infected cells were harvested and resuspended in 500 μ L binding buffer and stained with 5 μ L annexin V-fluorescein isothiocyanate (FITC) and 5 μ L propidium iodide (PI) of BD PharMingen apoptosis detection kit (BD Biosciences, San Diego, CA, USA) for 15 min in the dark. Annexin V⁻/PI⁻ cell populations were defined as living cells, Annexin V⁺/PI⁻ cell populations as viable apoptosis cells, and annexin V⁺/PI⁺ cell populations as non-viable apoptosis cells.

For analysis of immune cell populations in tumor, tumor cells were prepared as described above. The tumor cells were then pretreated

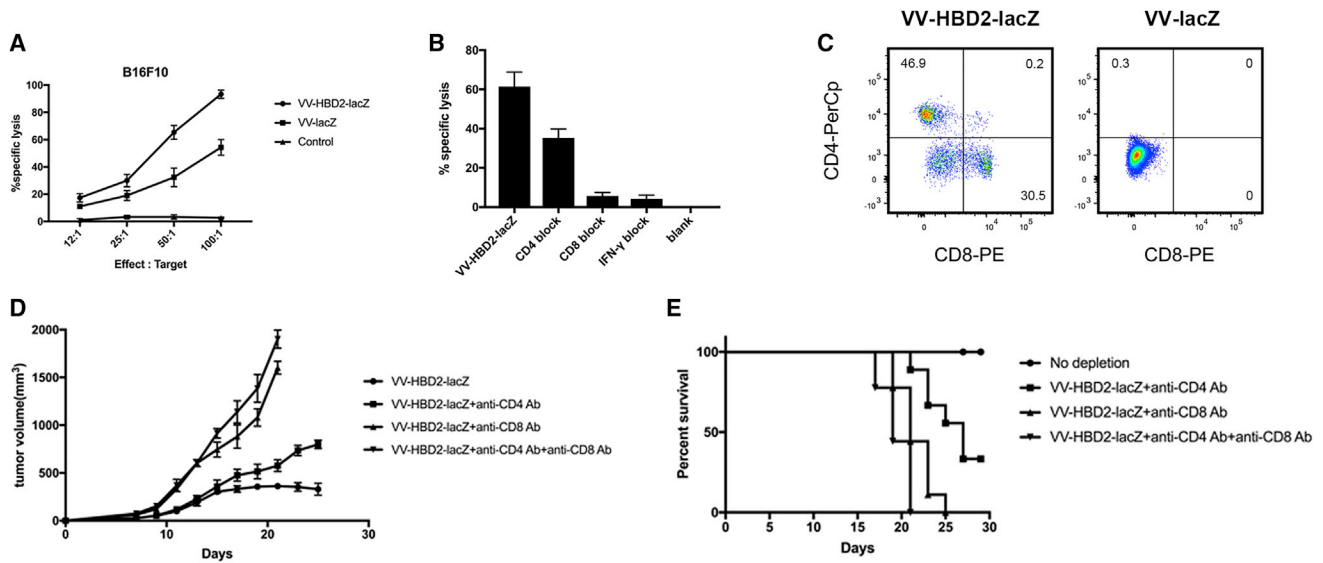


Figure 6. VV-HBD2-lacZ Enhances Intratumoral Cytotoxic T Lymphocyte Immunity

(A) Splenocytes from treated mice were cocultured with B16F10 cells for 24 h at different E:T ratios in a 96-well plate. The supernatant from each well was harvested, and cytolytic activity was tested by CCK-8 assay. (B) Five micrograms monoclonal anti-mouse CD4 or CD8 or IFN- γ were added into the above 96-well plate for the blocking assay. (C) Single-tumor cell from treated mice was stained with anti-mouse CD4-PerCP and CD8-PE. Percentage of cells is shown. (D) We performed antibody depletion experiments. Mice were sacrificed when the tumor reached 2000 mm³. Tumors were removed and weighed. (E) The percentage survival of mice in the antibody depletion experiments. IFN, interferon; PerCP, peridinin-chlorophyll-protein complex; PE, phycoerythrin.

with fragment crystallizable region (Fc) blocker and stained with anti-CD11c, anti-CD45RA, B220, anti-CD4, and anti-CD8.

All samples were run using BD FACScalibur flow cytometer (BD Biosciences, Franklin Lakes, NJ, USA) and analyzed using Flowjo software (Tree Star, Ashland, OR, USA).

Cytotoxicity T Cell Assay

The splenocytes were prepared as described above. Different numbers of splenocytes were co-cultured with 1×10^4 /well B16F10 cells for 24 h in 96-well plates. The effector-to-target cell ratios were 12:1, 25:1, 50:1, and 100:1 in quintuplicate. After incubation for 24 h, supernatants were harvested for cytokine-release assay. Cells in 96-well plates were washed twice with PBS, and CCK-8 solution was added to each well according to the manufacturer's instructions. The OD value was measured using a microplate reader (Bio-Tek, Hercules, CA, USA) at 450 nm after an hour of incubation. The percentage-specific lysis was calculated by $(1 - [\text{co-culture group OD} - \text{blank group OD}] / (\text{maximum kill group OD} - \text{blank group OD})) \times 100\%$.

In the effector lymphocyte blocking assay, 5 mg/well anti-mouse CD4 or CD8 antibodies (BD Biosciences, San Diego, CA) were added.

Statistical Analysis

All the data were obtained from at least three independent experiments and the data are presented as mean values \pm SD. Statistical analyses were carried out using GraphPad Prism (La Jolla, CA,

USA). Significance for comparison between groups was determined using one-way ANOVA test with Bonferroni correction for multiple comparisons. Differences in tumor growth were analyzed using two-tailed Student's *t* test. Differences were considered statistically significant when **p* < 0.05; ***p* < 0.01; ****p* < 0.005.

AUTHOR CONTRIBUTIONS

Conceptualization, H.Y. and T.S.; Methodology, H.Y., T.S., and Y.L.; Formal Analysis, T.S. and M.W.; Investigation, T.S. and M.W.; Writing – Original Draft, T.S.; Writing – Review & Editing, H.Y., Y.L., and T.S.; Funding Acquisition, H.Y. and T.X.; Resources, H.Y. and Y.L.; Supervision, H.Y. and T.X.

CONFLICTS OF INTEREST

The authors declare no competing interests..

ACKNOWLEDGMENTS

This work was supported by grants from the Natural Science Foundation of Zhejiang Province (no. LGF19H160032 and no. LZ16H160001) and the key programs of the National Natural Science Foundation of China (no. 81730108).

REFERENCES

1. Ferlay, J., Soerjomataram, I., Dikshit, R., Eser, S., Mathers, C., Rebelo, M., Parkin, D.M., Forman, D., and Bray, F. (2015). Cancer incidence and mortality worldwide: sources, methods and major patterns in GLOBOCAN 2012. *Int. J. Cancer* 136, E359–E386.

2. McGuire, S. (2016). World Cancer Report 2014. Geneva, Switzerland: World Health Organization, International Agency for Research on Cancer, WHO Press, 2015. *Adv. Nutr.* 7, 418–419.
3. Bahreyni, A., Ghorbani, E., Fuji, H., Ryzhikov, M., Khazaei, M., Erfani, M., Avan, A., Hassanian, S.M., and Azadmanesh, K. (2019). Therapeutic potency of oncolytic virotherapy-induced cancer stem cells targeting in brain tumors, current status, and perspectives. *J. Cell. Biochem.* 120, 2766–2773.
4. Alberts, P., Tilgase, A., Rasa, A., Bandere, K., and Venskus, D. (2018). The advent of oncolytic virotherapy in oncology: The Rigvir® story. *Eur. J. Pharmacol.* 837, 117–126.
5. Greig, S.L. (2016). Talimogene Laherparepvec: First Global Approval. *Drugs* 76, 147–154.
6. Conry, R.M., Westbrook, B., McKee, S., and Norwood, T.G. (2018). Talimogene laherparepvec: First in class oncolytic virotherapy. *Hum. Vaccin. Immunother.* 14, 839–846.
7. Mell, L.K., Brumund, K.T., Daniels, G.A., Advani, S.J., Zakeri, K., Wright, M.E., Onyeama, S.J., Weisman, R.A., Sanghvi, P.R., Martin, P.J., and Szalay, A.A. (2017). Phase I Trial of Intravenous Oncolytic Vaccinia Virus (GL-ONC1) with Cisplatin and Radiotherapy in Patients with Locoregionally Advanced Head and Neck Carcinoma. *Clin. Cancer Res.* 23, 5696–5702.
8. Hwang, T.H., Moon, A., Burke, J., Ribas, A., Stephenson, J., Breitbach, C.J., Daneshmand, M., De Silva, N., Parato, K., Diallo, J.S., et al. (2011). A mechanistic proof-of-concept clinical trial with JX-594, a targeted multi-mechanistic oncolytic poxvirus, in patients with metastatic melanoma. *Mol. Ther.* 19, 1913–1922.
9. Parato, K.A., Breitbach, C.J., Le Boeuf, F., Wang, J., Storbeck, C., Ilkow, C., Diallo, J.S., Falls, T., Burns, J., Garcia, V., et al. (2012). The oncolytic poxvirus JX-594 selectively replicates in and destroys cancer cells driven by genetic pathways commonly activated in cancers. *Mol. Ther.* 20, 749–758.
10. Mejias-Pérez, E., Carreño-Fuentes, L., and Esteban, M. (2017). Development of a Safe and Effective Vaccinia Virus Oncolytic Vector WR-Δ4 with a Set of Gene Deletions on Several Viral Pathways. *Mol. Ther. Oncolytics* 8, 27–40.
11. Fang, L., Cheng, Q., Li, W., Liu, J., Li, L., Xu, K., and Zheng, J. (2014). Antitumor activities of an oncolytic adenovirus equipped with a double siRNA targeting Ki67 and hTERT in renal cancer cells. *Virus Res.* 181, 61–71.
12. Breitbach, C.J., Parato, K., Burke, J., Hwang, T.H., Bell, J.C., and Kirn, D.H. (2015). Pexa-Vec double agent engineered vaccinia: oncolytic and active immunotherapeutic. *Curr. Opin. Virol.* 13, 49–54.
13. Thorne, S.H., Hwang, T.H., O’Gorman, W.E., Bartlett, D.L., Sei, S., Kanji, F., Brown, C., Werier, J., Cho, J.H., Lee, D.E., et al. (2007). Rational strain selection and engineering creates a broad-spectrum, systemically effective oncolytic poxvirus, JX-963. *J. Clin. Invest.* 117, 3350–3358.
14. Merrick, A.E., Ilett, E.J., and Melcher, A.A. (2009). JX-594, a targeted oncolytic poxvirus for the treatment of cancer. *Curr. Opin. Investig. Drugs* 10, 1372–1382.
15. Liu, T.C., Hwang, T., Park, B.H., Bell, J., and Kirn, D.H. (2008). The targeted oncolytic poxvirus JX-594 demonstrates antitumoral, antivascular, and anti-HBV activities in patients with hepatocellular carcinoma. *Mol. Ther.* 16, 1637–1642.
16. Pazgier, M., Hoover, D.M., Yang, D., Lu, W., and Lubkowski, J. (2006). Human beta-defensins. *Cell. Mol. Life Sci.* 63, 1294–1313.
17. Boniotto, M., Jordan, W.J., Eskdale, J., Tossi, A., Antcheva, N., Crovella, S., Connell, N.D., and Gallagher, G. (2006). Human beta-defensin 2 induces a vigorous cytokine response in peripheral blood mononuclear cells. *Antimicrob. Agents Chemother.* 50, 1433–1441.
18. Biragyn, A., Ruffini, P.A., Leifer, C.A., Klyushnchenkova, E., Shakhov, A., Chertov, O., Shirakawa, A.K., Farber, J.M., Segal, D.M., Oppenheim, J.J., and Kwak, L.W. (2002). Toll-like receptor 4-dependent activation of dendritic cells by beta-defensin 2. *Science* 298, 1025–1029.
19. Biragyn, A., Belyakov, I.M., Chow, Y.H., Dimitrov, D.S., Berzofsky, J.A., and Kwak, L.W. (2002). DNA vaccines encoding human immunodeficiency virus-1 glycoprotein 120 fusions with proinflammatory chemoattractants induce systemic and mucosal immune responses. *Blood* 100, 1153–1159.
20. Yang, D., Chertov, O., Bykovskaia, S.N., Chen, Q., Buffo, M.J., Shogan, J., Anderson, M., Schröder, J.M., Wang, J.M., Howard, O.M., and Oppenheim, J.J. (1999). Beta-defensins: linking innate and adaptive immunity through dendritic and T cell CCR6. *Science* 286, 525–528.
21. Huang, G.T., Zhang, H.B., Kim, D., Liu, L., and Ganz, T. (2002). A model for antimicrobial gene therapy: demonstration of human beta-defensin 2 antimicrobial activities in vivo. *Hum. Gene Ther.* 13, 2017–2025.
22. Breitbach, C.J., Burke, J., Jonker, D., Stephenson, J., Haas, A.R., Chow, L.Q., Nieva, J., Hwang, T.H., Moon, A., Patt, R., et al. (2011). Intravenous delivery of a multi-mechanistic cancer-targeted oncolytic poxvirus in humans. *Nature* 477, 99–102.
23. McFadden, G. (2005). Poxvirus tropism. *Nat. Rev. Microbiol.* 3, 201–213.
24. Yu, Q., Hu, N., and Ostrowski, M. (2009). Poxvirus tropism for primary human leukocytes and hematopoietic cells. *Methods Mol. Biol.* 515, 309–328.
25. Wein, L.M., Wu, J.T., and Kirn, D.H. (2003). Validation and analysis of a mathematical model of a replication-competent oncolytic virus for cancer treatment: implications for virus design and delivery. *Cancer Res.* 63, 1317–1324.
26. Lapteva, N., Aldrich, M., Rollins, L., Ren, W., Goltsova, T., Chen, S.-Y., and Huang, X.F. (2009). Attraction and activation of dendritic cells at the site of tumor elicits potent antitumor immunity. *Mol. Ther.* 17, 1626–1636.
27. Kirn, D.H., and Thorne, S.H. (2009). Targeted and armed oncolytic poxviruses: a novel multi-mechanistic therapeutic class for cancer. *Nat. Rev. Cancer* 9, 64–71.
28. Guse, K., Cerullo, V., and Hemminki, A. (2011). Oncolytic vaccinia virus for the treatment of cancer. *Expert Opin. Biol. Ther.* 11, 595–608.
29. Alculumbre, S., Raieli, S., Hoffmann, C., Chelbi, R., Danlos, F.X., and Soumelis, V. (2019). Plasmacytoid pre-dendritic cells (pDC): from molecular pathways to function and disease association. *Semin. Cell Dev. Biol.* 86, 24–35.
30. Gilliet, M., and Liu, Y.J. (2002). Generation of human CD8 T regulatory cells by CD40 ligand-activated plasmacytoid dendritic cells. *J. Exp. Med.* 195, 695–704.
31. Zhou, X., Michal, J.J., Zhang, L., Ding, B., Lunney, J.K., Liu, B., and Jiang, Z. (2013). Interferon induced IFIT family genes in host antiviral defense. *Int. J. Biol. Sci.* 9, 200–208.
32. McKenna, K., Beignon, A.S., and Bhardwaj, N. (2005). Plasmacytoid dendritic cells: linking innate and adaptive immunity. *J. Virol.* 79, 17–27.
33. Brewitz, A., Eickhoff, S., Dähling, S., Quast, T., Bedoui, S., Kroczeck, R.A., Kurts, C., Garbi, N., Barchet, W., Iannacone, M., et al. (2017). CD8⁺ T Cells Orchestrate pDC-XCR1⁺ Dendritic Cell Spatial and Functional Cooperativity to Optimize Priming. *Immunity* 46, 205–219.
34. Villadangos, J.A., and Young, L. (2008). Antigen-presentation properties of plasmacytoid dendritic cells. *Immunity* 29, 352–361.
35. Heatley, N.G. (1944). A method for the assay of penicillin. *Biochem. J.* 38, 61–65.
36. Qu, D., Wang, S., Cai, W., and Du, A. (2008). Protective effect of a DNA vaccine delivered in attenuated *Salmonella typhimurium* against *Toxoplasma gondii* infection in mice. *Vaccine* 26, 4541–4548.
37. Justus, C.R., Leffler, N., Ruiz-Echevarria, M., and Yang, L.V. (2014). In vitro cell migration and invasion assays. *J. Vis. Exp.* 2014, 51046.